VIBRATION CONTROL OF COMPOSITE THICK SHELLS USING MAGNETOSTRICTIVE MATERIAL AND HIGHER ORDER SHEAR DEFORMATION THEORY

K. Narendra* and S.C. Pradhan*

Abstract

Analytical solutions of laminated composite shells with embedded actuating layers are presented in this study. The actuating layers are used to control natural vibration of laminated composite shell panels. The first order shear deformation theory (FSDT) and higher order shear deformation theory (HSDT) for shells are used to represent the shell kinematics and equations of motion. The exact solution for symmetric laminated shells with embedded actuating layers under simply supported boundary conditions is obtained using the Navier solution procedure. Negative velocity feedback control is used. The parametric effect of the position of the magnetostrictive layers, material properties and control parameters on the vibration suppression are investigated in detail. It is found that (i) the shortest vibration suppression time is achieved by placing the actuating layers farthest from the neutral axis (ii) using thinner smart material layers leads to better vibration attenuation characteristics and, (iii) the vibration suppression time is longer for a lower value of the feedback control coefficient. For thicker shells HSDT predicts larger amplitude of vibration and longer vibration suppression time as compared to FSDT predictions.

Keywords : Composite material, Higher order shear deformation, Vibration suppression, Shell

Nomenclature

$A_{31}, A_{32}, B_{31}, B_{32}, C_{31}, C_{32}$ = magnetostrictive coefficients

α , β = positive real number

α_1, α_2 = surface metrics

$\varepsilon_1, \varepsilon_2, \varepsilon_6, \gamma_4, \gamma_5$ = total strains

$\varepsilon_1^0, \varepsilon_2^0, \varepsilon_6^0, \gamma_4^0, \gamma_5^0$ = strains from classical shell theory

$\varepsilon_1^1, \varepsilon_2^1, \varepsilon_6^1, \gamma_4^1, \gamma_5^1, \varepsilon_1^2, \varepsilon_2^2, \varepsilon_6^2$ = strains from HSDT

ξ_1, ξ_2, ζ = orthogonal curvilinear co-ordinates

λ = eigen value

λ_0 = arbitrary constant

ϕ_1, ϕ_2 = rotational displacements

ν_m = Poissons ratio of magnetostrictive material

$\rho^{(K)}$ = density of k^{th} layer

ρ_m = density of magnetostrictive material

$\sigma_1, \sigma_2, \tau_4, \tau_5, \sigma_6$ = stress components

ω_d = damping frequency

a = length of the shell

b = breadth of the shell

b_c = coil width

$C(t)$ = control gain

d_k = material constant

dA_1, dA_2 = elementary areas across the thickness of the shell

* Department of Aerospace Engineering, Indian Institute of Technology Kharagpur, Kharagpur-721 302, West Bengal, India, Email : scp@aero.iitkgp.ernet.in

Manuscript received on 20 Nov 2008; Paper reviewed, revised, re-revised and accepted as a Full Length Contributed Paper on 07 Sep 2009

ds = square of the distance on the middle surface
dS = square of the distance
$e_{31}^{(k)}, e_{32}^{(k)}, e_{36}^{(k)}$ = magnetostrictive material properties of k^{th} layer
g_1, g_2 = tangents to ξ_1, ξ_2
h = thickness of the shell
h_l = thickness of each composite layer
h_m = thickness of magnetostrictive layer
k_c = magnetostrictive coil constant
m, m_1, m_2, n = positive integers
n_c = number of coil turns
q = uniformly distributed load in the transverse direction
r = position vector on the middle surface
r_c = coil radius
t = suppression time
z = thickness co-ordinate
$[\ ]^0$ = contribution due to classical shell theory
$[\ ]^M$ = contribution due to magnetostrictive layer
$A_{ij}, B_{ij}, D_{ij}, E_{ij}, F_{ij}, H_{ij}$ = stiffness coefficients of composite material
C_1, C_2 = constants which depend on thickness of the shell
E_m = Youngs modulus of magnetostrictive material
H = magnetic field intensity
I = coil current intensity
$I_1, I_2, I_3, I_4, I_5, I_6, I_7$ = moment of inertia
$\bar{I}_i, \bar{J}_i, i = 1, 5$ = terms which depend on inertia terms
L_1, L_2, L_3 = lame coefficients
M_1, M_2, M_6 = moments applied on the edges of the shell
M^M = moments due to the magnetostrictive layer
N = number of layers assumed for computation
N_1, N_2, N_6 = forces applied on the edges of the shell
N^M = forces due to the magnetostrictive layer
Q_1, Q_2 = shear forces applied on the edges of the shell
K_1, K_2 = shear forces
$Q_{ij}^{(k)}$ = stiffness coefficients of k^{th} layer
R = position vector of arbitrary point
R_1, R_2 = principal radii of curvature of the middle surface of the shell
R_n = positive real number
S_{ij}, C_{ij}, M_{ij} = coefficients of stiffness, damping and mass matrices
$\bar{S}_{ij}$ = coefficients of solution matrix
T_S = suppression time ratio
W_{max} = maximum amplitude in transverse direction
Z_m = transverse location of magnetostrictive layer in the shell

Introduction

A number of materials have been used in sensor/actuator applications. Piezoelectric materials, magnetostrictive materials, shape memory alloys, and electro-rheological fluids have all been integrated with aerospace structures to make smart structures. Among these materials piezoelectric, electrostrictive and magnetostrictive materials have the capability to serve as both sensors and actuators. Piezoelectric materials exhibit a linear relationship between the electric field and strains for low field values (up to 100V/mm). This relationship is nonlinear for large fields, and the material exhibits hysteresis [1]. Further, piezoelectric materials show dielectric aging and hence lack reproducibility of strains, i.e. a drift from zero state of strain is observed under cyclic electric field applications [2].

Crawley and Luis [3] demonstrated the feasibility of using piezoelectric actuators for free vibration reduction of a cantilever beam. Baz, et al. [4] investigated vibration control using shape memory alloy and carried out their characterization. Choi et al., [5] demonstrated the vibration reduction effects of electro rheological fluid actuators in a composite beam.

An ideal actuator, for distributed embedded application, should have high energy density, negligible weight and point excitation with a wide frequency bandwidth. Terfenol-D, a magnetostrictive material, has the characteristics of being able to produce strains up to 2000 μm and the energy density as high as 25000 Jm^{-3} in response to a magnetic field. Goodfriend and Shoop [6] reviewed the material properties of Terfenol-D with regard to its use in vibration isolation. Bryant et al. [7] presented experimental results of a magnetostrictive Terfenol-D rod used in dual capacity of passive structural support element and an active vibration control actuator. Friedmann et al. [8] used

magnetostrictive material Terfenol-D in high speed helicopter rotors and studied the vibration reduction characteristics. Anjanaappa and Bi [9,10] investigated the feasibility of using embedded magnetostrictive mini actuators for smart structure applications, such as vibration suppression of beams. A self-sensing magnetostrictive actuator design based on a linear model of magnetostrictive transduction for Terfenol-D was developed and analyzed by Pratt and Flatau [11]. Eda et al. [12] and Krishna Murty et al. [13,14] proposed magnetostrictive actuators that take advantage of the ease with which the actuators can be embedded and remote excitation capability of magnetostrictive particles as actuators for smart structures. Reddy [15], Reddy and Barbosa [16], Pradhan et al. [17], Marfia et al. [18] and Reddy and Liu [19] presented finite element formulations and analytical solutions for simply supported boundary conditions of laminated composite beams and plates with embedded active layers.

Reddy [20-23] reported higher order theory and its effects on composite materials. Lee and Guo [24] studied non-linear vibration suppression of a composite panel. Song et al. [25] presented a review article about vibration control of civil structures using smart materials. Pradhan [26] studied vibration suppression of FGM (Functionally Graded Material) structures. Zhang and Shen [27] reported vibration suppression of laminated plates with piezoelectric fiber-reinforced composite layers. However, there is very little information is available on higher order shear deformation studies of smart composite shells.

In the present study vibration control of smart composite shells is studied using the higher order shear deformation theory. Exact solutions are developed for simply supported doubly curved composite shells with embedded magnetostrictive layers. This closed form solution exists for the shells. A simple negative velocity feedback control is used to actively control the dynamic response of the structure through a closed loop control. Numerical results of vibration suppression effect for various locations of the magnetostrictive layers, material properties, and control parameters are presented. Influence of HSDT on the thick composite shells is also investigated.

Theoretical Formulation

Kinematic Description

Figure 1a contains a differential element of a doubly curved shell element with constant curvatures along two coordinate directions (ξ_1, ξ_2), where (ξ_1, ξ_2, ζ) denote the orthogonal curvilinear coordinates such that ξ_1 and ξ_2 curves are the lines of curvature on the middle surface ($\zeta = 0$). Thus, the doubly curved shell panel considered here, the lines of the principal curvature coincide with the coordinate lines. The values of the principal radii of curvature of the middle surface are denoted by R_1 and R_2. The position vector of a point (ξ_1, ξ_2, 0) on the middle surface is denoted by $\mathbf{r}$, and the position of an arbitrary point (ξ_1, ξ_2, ζ) is denoted by $\mathbf{R}$ (Fig.2). The square of the distance ds between points (ξ_1, ξ_2, 0) and ($\xi_1 + d\xi_1$, $\xi_2 + d\xi_2$, 0) is determined by

$$(ds)^2 = d\,\mathbf{r} \,.\, d\,\mathbf{r} = \alpha_1^2 (d\,\xi_1)^2 + \alpha_2^2 (d\,\xi_2)^2 \tag{1}$$

in which $d\,\mathbf{r} = \boldsymbol{g}_1\, d\,\xi_1 + \boldsymbol{g}_2\, d\,\xi_2$ the vectors $\mathbf{g}_1$ and $\mathbf{g}_2$ ($\boldsymbol{g}_i = \dfrac{\partial \boldsymbol{r}}{\partial \xi_i}$) are tangent to the ξ_1 and ξ_2 coordinate lines and α_1 and α_2 are the surface metrics

$$\alpha_1^2 = \boldsymbol{g}_1 \cdot \boldsymbol{g}_1, \quad \alpha_2^2 = \boldsymbol{g}_2 \cdot \boldsymbol{g}_2 \tag{2}$$

The square of the distance dS between (ξ_1, ξ_2, ζ) and ($\xi_1 + d\xi_1$, $\xi_2 + d\xi_2$, $\zeta + d\zeta$) is given by

$$(dS)^2 = d\,\mathbf{R} \,.\, d\,\mathbf{R} = L_1^2 (d\,\xi_1)^2 + L_2^2 (d\,\xi_2)^2 + L_3^2 (d\,\zeta)^2 \tag{3}$$

in which $d\mathbf{R} = \left(\dfrac{\partial \mathbf{R}}{\partial \xi_1}\right) d\,\xi_1 + \left(\dfrac{\partial \mathbf{R}}{\partial \xi_2}\right) d\,\xi_2 + \left(\dfrac{\partial \mathbf{R}}{\partial \zeta}\right) d\zeta$ and L_1, L_2 and L_3 are the Lame' coefficients

$$L_1 = \alpha_1 \left(1 + \frac{\zeta}{R_1}\right), \quad L_2 = \alpha_2 \left(1 + \frac{\zeta}{R_2}\right), \quad L_3 = 1 \tag{4}$$

Displacement Field

We assume the following form of the displacement field that is consistent with the assumptions of a thick shell theory as explained in Reddy and Liu [19].

$$\bar{u}_1 (\xi_1, \xi_2, \zeta, t) = \frac{L_1}{\alpha_1} u_1 (\xi_1, \xi_2, t) + \zeta \phi_1 (\xi_1, \xi_2, t) - c_1 \zeta^3 \left(\phi_1 + \frac{\partial u_3}{\alpha_1 \partial \xi_1}\right)$$

$$\bar{u}_2(\xi_1, \xi_2, \zeta, t) = \frac{L_2}{\alpha_2} u_2(\xi_1, \xi_2, t) + \zeta\phi_2(\xi_1, \xi_2, t) - c_1\zeta^3\left(\phi_2 + \frac{\partial u_3}{\alpha_1 \partial \xi_2}\right)$$
$$\bar{u}_3(\xi_1, \xi_2, \zeta, t) = u_3(\xi_1, \xi_2, t) \tag{5}$$

where

$$\frac{1}{\partial x_i} = \frac{1}{\alpha_i}\frac{1}{\partial \xi_i} (i = 1, 2) \tag{6}$$

$(\bar{u}_1, \bar{u}_2, \bar{u}_3)$ are the displacements of a point (ξ_1, ξ_2, ζ) along the (ξ_1, ξ_2, ζ) coordinates; and (u_1, u_2, u_3) are displacements of a point $(\xi_1, \xi_2, 0)$ on the mid surface of the shell. Substituting equation (5) into strain-displacement relations for the third-order shear deformation theory, one obtains

$$\begin{Bmatrix}\varepsilon_1\\ \varepsilon_2\\ \varepsilon_6\end{Bmatrix} = \begin{Bmatrix}\varepsilon_1^0\\ \varepsilon_2^0\\ \varepsilon_6^0\end{Bmatrix} + \zeta\begin{Bmatrix}\varepsilon_1^1\\ \varepsilon_2^1\\ \varepsilon_6^1\end{Bmatrix} + \zeta^3\begin{Bmatrix}\varepsilon_1^2\\ \varepsilon_2^2\\ \varepsilon_6^2\end{Bmatrix}$$
$$\begin{Bmatrix}\gamma_4\\ \gamma_5\end{Bmatrix} = \begin{Bmatrix}\gamma_4^0\\ \gamma_5^0\end{Bmatrix} + \zeta^2\begin{Bmatrix}\gamma_4^1\\ \gamma_5^1\end{Bmatrix} \tag{7}$$

where

$$\begin{Bmatrix}\varepsilon_1^0\\ \varepsilon_2^0\\ \varepsilon_6^0\end{Bmatrix} = \begin{Bmatrix}\dfrac{\partial u_1}{\partial x_1} + \dfrac{1}{R_1}u_3\\ \dfrac{\partial u_2}{\partial x_2} + \dfrac{1}{R_2}u_3\\ \dfrac{\partial u_2}{\partial x_1} + \dfrac{\partial u_1}{\partial x_2}\end{Bmatrix}$$

$$\begin{Bmatrix}\varepsilon_1^1\\ \varepsilon_2^1\\ \varepsilon_6^1\end{Bmatrix} = \begin{Bmatrix}\dfrac{\partial \phi_1}{\partial x_1}\\ \dfrac{\partial \phi_2}{\partial x_2}\\ \dfrac{\partial \phi_2}{\partial x_1} + \dfrac{\partial \phi_1}{\partial x_2}\end{Bmatrix}$$

$$\begin{Bmatrix}\varepsilon_1^2\\ \varepsilon_2^2\\ \varepsilon_6^2\end{Bmatrix} = -C_1\begin{Bmatrix}\dfrac{\partial \phi_1}{\partial x_1} + \dfrac{\partial^2 u_3}{\partial x_1^2}\\ \dfrac{\partial \phi_2}{\partial x_2} + \dfrac{\partial^2 u_3}{\partial x_2^2}\\ \dfrac{\partial \phi_2}{\partial x_1} + \dfrac{\partial \phi_1}{\partial x_2} + 2\dfrac{\partial^2 u_3}{\partial x_1 \partial x_2}\end{Bmatrix}$$

$$\begin{Bmatrix}\gamma_4^0\\ \gamma_5^0\end{Bmatrix} = \begin{Bmatrix}\phi_2 + \dfrac{\partial u_3}{\partial x_2}\\ \phi_1 + \dfrac{\partial u_3}{\partial x_1}\end{Bmatrix}$$

$$\begin{Bmatrix}\gamma_4^1\\ \gamma_5^1\end{Bmatrix} = -C_2\begin{Bmatrix}\phi_2 + \dfrac{\partial u_3}{\partial x_2}\\ \phi_1 + \dfrac{\partial u_3}{\partial x_1}\end{Bmatrix} \tag{8}$$

and (ϕ_1, ϕ_2) are rotations of a transverse normal line about the ξ_2 and ξ_1 coordinate axes, respectively.

$$\phi_1 = -\frac{\partial u_3}{\partial \xi_1}, \quad \phi_2 = -\frac{\partial u_3}{\partial \xi_2} \tag{9}$$

Constants C_1 and C_2 are defined as

$$C_1 = \frac{4}{3h^2}, \; C_2 = 3C_1 \tag{10}$$

Constitutive Relations

Suppose that the shell is composed of N orthotropic layers stacked on each other, with each layer principal material 1 axis oriented at an angle θ_k from the shell x_1 coordinate in the counterclockwise sense. The stress-strain relations of the k^{th} lamina, whether structural layer or actuating/sensing layer, in the shell coordinate system are given as

$$\begin{Bmatrix} \sigma_1 \\ \sigma_2 \\ \tau_4 \\ \tau_5 \\ \sigma_6 \end{Bmatrix}^{(k)} = \begin{bmatrix} \overline{Q}_{11} & \overline{Q}_{12} & 0 & 0 & \overline{Q}_{16} \\ \overline{Q}_{12} & \overline{Q}_{22} & 0 & 0 & \overline{Q}_{26} \\ 0 & 0 & \overline{Q}_{44} & \overline{Q}_{45} & 0 \\ 0 & 0 & \overline{Q}_{45} & \overline{Q}_{55} & 0 \\ \overline{Q}_{16} & \overline{Q}_{26} & 0 & 0 & \overline{Q}_{66} \end{bmatrix}^{(k)} \begin{Bmatrix} \varepsilon_1 \\ \varepsilon_2 \\ \gamma_4 \\ \gamma_5 \\ \varepsilon_6 \end{Bmatrix}^{k} - \zeta \begin{Bmatrix} \overline{e}_{31} \\ \overline{e}_{32} \\ 0 \\ 0 \\ \overline{e}_{36} \end{Bmatrix}^{(k)} H \tag{11}$$

where $\overline{Q}_{ij}$ are the transformed stiffnesses and $Q_{ij}^{(k)}$ are the lamina stiffnesses referred to the principal material coordinates of the k^{th} lamina.

$$\overline{Q}_{11} = Q_{11}\cos^4\theta + 2(Q_{12}+2Q_{66})\sin^2\theta\cos^2\theta + Q_{22}\sin^4\theta$$

$$\overline{Q}_{12} = (Q_{11}+Q_{22}-4Q_{66})\sin^2\theta\cos^2\theta + Q_{12}(\sin^4\theta+\cos^4\theta)$$

$$\overline{Q}_{22} = Q_{11}\sin^4\theta + 2(Q_{12}+2Q_{66})\sin^2\theta\cos^2\theta + Q_{22}\cos^4\theta$$

$$\overline{Q}_{16} = (Q_{11}-Q_{12}-2Q_{66})\sin\theta\cos^3\theta + (Q_{12}-Q_{22}+2Q_{66})\sin^3\theta\cos\theta$$

$$\overline{Q}_{26} = (Q_{11}-Q_{12}-2Q_{66})\sin^3\theta\cos\theta + (Q_{12}-Q_{22}+2Q_{66})\sin\theta\cos^3\theta$$

$$\overline{Q}_{66} = (Q_{11}+Q_{22}-2Q_{12}-2Q_{66})\sin^2\theta\cos^2\theta + Q_{66}(\sin^4\theta+\cos^4\theta)$$

$$\overline{Q}_{44} = Q_{44}\cos^2\theta + Q_{55}\sin^2\theta$$

$$\overline{Q}_{45} = (Q_{55}-Q_{44})\cos\theta\sin\theta$$

$$\overline{Q}_{55} = Q_{55}\cos^2\theta + Q_{44}\sin^2\theta \tag{12}$$

and

$$Q_{11} = \frac{E_1}{1-\nu_{12}\nu_{21}},\quad Q_{12} = \frac{\nu_{12}E_2}{1-\nu_{12}\nu_{21}},\quad Q_{22} = \frac{E_2}{1-\nu_{12}\nu_{21}}$$

$$Q_{66} = G_{12},\quad Q_{44} = G_{23},\quad Q_{55} = G_{13} \tag{13}$$

The superscript k on Q_{ij}, θ, as well as on the engineering constants E_1, E_2, ν_{12} and so on are omitted for brevity. In equation (11), H denotes the intensity of the magnetic field and $\overline{e}_{ij}$ are the magnetostrictive material coefficients.

$$\overline{e}_{31} = e_{31}\cos^2\theta + e_{32}\sin^2\theta$$
$$\overline{e}_{32} = e_{32}\cos^2\theta + e_{31}\sin^2\theta$$
$$\overline{e}_{36} = (e_{31}-e_{32})\sin\theta\cos\theta \tag{14}$$

Feedback Control

A velocity feedback control is used in the present study. In the velocity feedback control, the magnetic field intensity H is expressed in terms of coil current $I(\xi_1, \xi_2, t)$

$$H(\xi_1, \xi_2, t) = k_c\, I(\xi_1, \xi_2, t) \tag{15}$$

Current I is related to the transverse velocity $\dot{u}_3$ component as

$$I(\xi_1, \xi_2, t) = c(t)\frac{\partial u_3}{\partial t} \tag{16}$$

where k_c is the magnetic coil constant and is related to the number of coil turns n_c coil width b_c, and coil radius r_c

$$k_c = \frac{n_c}{\sqrt{b_c^2 + 4r_c^2}} \tag{17}$$

The parameter *c(t)* is known as the control gain.

Equations of Motion

The governing equations of motion is being derived from the dynamic version of the principle of virtual work for the laminated shell. By integrating the displacement gradients by parts and setting the coefficients of δu_1, δu_2, δu_3, $\delta\phi_1$ and $\delta\phi_2$ to zero separately (the moment terms in the first two equations are omitted) we get

$$\frac{\partial N_1}{\partial x_1} + \frac{\partial N_6}{\partial x_2} = \bar{I}_1\frac{\partial^2 u_1}{\partial t^2} + \bar{I}_2\frac{\partial^2 \phi_1}{\partial t^2} - \bar{I}_3\frac{\partial^2 u_3}{\partial t^2}$$

$$\frac{\partial N_6}{\partial x_1} + \frac{\partial N_2}{\partial x_2} = \bar{J}_1 \frac{\partial^2 u_2}{\partial t^2} + \bar{J}_2 \frac{\partial^2 \phi_2}{\partial t^2} - \bar{J}_3 \frac{\partial^2 u_3}{\partial t^2}$$

$$\frac{\partial Q_1}{\partial x_1} + \frac{\partial Q_2}{\partial x_2} - C_2 \left(\frac{\partial K_1}{\partial x_1} + \frac{\partial K_2}{\partial x_2} \right) + C_1 \left(\frac{\partial^2 P_1}{\partial x_1^2} + 2 \frac{\partial^2 P_6}{\partial x_1 \partial x_2} + \frac{\partial^2 P_2}{\partial x_2^2} \right)$$

$$- \frac{N_1}{R_1} - \frac{N_2}{R_2} + q = \bar{I}_3 \frac{\partial^3 u_1}{\partial x_1 \partial t^2} + \bar{I}_5 \frac{\partial^3 \phi_1}{\partial x_1 \partial t^2} + \bar{J}_3 \frac{\partial^3 u_2}{\partial x_2 \partial t^2}$$

$$+ \bar{J}_5 \frac{\partial^3 \phi_2}{\partial x_2 \partial t^2} + I_1 \frac{\partial^2 u_3}{\partial t^2} - C_1^2 I_7 \left(\frac{\partial^4 u_3}{\partial x_1^2 \partial t^2} + \frac{\partial^4 u_3}{\partial x_2^2 \partial t^2} \right)$$

$$\frac{\partial M_1}{\partial x_1} + \frac{\partial M_6}{\partial x_2} - Q_1 + C_2 K_1 - C_1 \left(\frac{\partial P_1}{\partial x_1} + \frac{\partial P_6}{\partial x_2} \right)$$

$$= \bar{I}_2 \frac{\partial^2 u_1}{\partial t^2} + \bar{I}_4 \frac{\partial^2 \phi_1}{\partial t^2} - \bar{I}_5 \frac{\partial^3 u_3}{\partial x_1 \partial t^2}$$

$$\frac{\partial M_6}{\partial x_1} + \frac{\partial M_2}{\partial x_2} - Q_2 + C_2 K_2 - C_1 \left(\frac{\partial P_6}{\partial x_1} + \frac{\partial P_2}{\partial x_2} \right)$$

$$= \bar{J}_2 \frac{\partial^2 u_2}{\partial t^2} + \bar{J}_4 \frac{\partial^2 \phi_2}{\partial t^2} - \bar{J}_5 \frac{\partial^3 u_3}{\partial x_2 \partial t^2} \qquad (18)$$

where

$$(N_i, M_i, P_i) = \sum_{k=1}^{N} \int_{\zeta k}^{\zeta k+1} \sigma_i^{(k)} (1, \zeta, \zeta^3)\, d\zeta \; (i = 1, 2, 6)$$

$$(Q_1, K_1) = \sum_{k=1}^{N} \int_{\zeta k}^{\zeta k+1} \sigma_5^{(k)} (1, \zeta^2)\, d\zeta$$

$$(Q_2, K_2) = \sum_{k=1}^{N} \int_{\zeta k}^{\zeta k+1} \sigma_4^{(k)} (1, \zeta^2)\, d\zeta \qquad (19)$$

$$\bar{I}_1 = I_1 + \frac{2}{R_1} I_2$$

$$\bar{J}_1 = I_1 + \frac{2}{R_2} I_2$$

$$\bar{I}_2 = I_3 + \frac{1}{R_1} I_3 - C_1 \left(I_4 + \frac{1}{R_1} I_5 \right)$$

$$\bar{J}_2 = I_3 + \frac{1}{R_2} I_3 - C_1 \left(I_4 + \frac{1}{R_2} I_5 \right)$$

$$\bar{I}_3 = C_1 \left(I_4 + \frac{1}{R_1} I_5 \right)$$

$$\bar{J}_3 = C_1 \left(I_4 + \frac{1}{R_2} I_5 \right)$$

$$\bar{I}_4 = I_3 - C_1 (2 I_5 - C_1 I_7)$$

$$\bar{J}_4 = \bar{I}_4$$

$$\bar{I}_5 = C_1 (2 I_5 - C_1 I_7)$$

$$\bar{J}_5 = \bar{I}_5 \qquad (20)$$

The inertia terms are defined as

$$(I_1, I_2, I_3, I_4, I_5, I_7) = \sum_{k=1}^{N} \int_{\zeta k}^{\zeta k+1} \rho^{(k)} (1, \zeta, \zeta^2, \zeta^3, \zeta^4, \zeta^6)\, d\zeta \qquad (21)$$

where $\rho^{(k)}$ being the density of the k^{th} layer and N is the number of layers in the laminate.

Laminate Constitutive Equation

Using equations (7) and (11) in equation (19) we get the following constitutive equations for the actuator embedded laminate

$$\begin{Bmatrix} \{N\} \\ \{M\} \\ \{P\} \end{Bmatrix} = \begin{bmatrix} [A] & [B] & [E] \\ [B] & [D] & [F] \\ [E] & [F] & [H] \end{bmatrix} \begin{Bmatrix} \{\varepsilon^0\} \\ \{\varepsilon^1\} \\ \{\varepsilon^2\} \end{Bmatrix} - \begin{Bmatrix} \{N\} \\ \{M\} \\ \{P\} \end{Bmatrix}^M \qquad (22)$$

$$\begin{Bmatrix} \{Q\} \\ \{K\} \end{Bmatrix} = \begin{bmatrix} [A] & [D] \\ [D] & [F] \end{bmatrix} \begin{Bmatrix} \gamma^0 \\ \gamma^1 \end{Bmatrix} - \begin{Bmatrix} \{Q\} \\ \{K\} \end{Bmatrix}^M \tag{23}$$

where the laminate stiffness coefficients (A_{ij}, B_{ij}, D_{ij}, E_{ij}, F_{ij}, H_{ij} for i,j = 1, 2, 6) are defined by

$$(A_{ij}, B_{ij}, D_{ij}, E_{ij}, F_{ij}, H_{ij}) = \sum_{k=1}^{N} \int_{\zeta k}^{\zeta k+1} \overline{Q}_{ij}^{(k)} \; (1, \zeta, \zeta^2, \zeta^3, \zeta^4, \zeta^6) \, d\zeta \tag{24}$$

and the laminate stiffness coefficients (A_{ij}, D_{ij}, F_{ij} for i,j = 4, 5) are defined by

$$(A_{ij}, D_{ij}, F_{ij}) = \sum_{k=1}^{N} \int_{\zeta k}^{\zeta k+1} \overline{Q}_{ij}^{(k)} \; (1, \zeta^2, \zeta^4) \, d\zeta \quad (i, j = 4, 5) \tag{25}$$

The magnetostrictive stress resultants $\{N_i^M\}$, $\{M_i^M\}$ and $\{K_i^M\}$ for (i = 1, 2) are defined as

$$\begin{Bmatrix} \{N_1^M\} \\ \{N_2^M\} \end{Bmatrix} = \sum_{k=m_1,m_2\ldots}^{N} \int_{\zeta k}^{\zeta k+1} \begin{Bmatrix} \{\overline{e}_{31}\} \\ \{\overline{e}_{32}\} \end{Bmatrix} H_\zeta \, d\zeta$$

$$= ck_c \sum_{k=m_1,m_2\ldots}^{N} \int_{\zeta k}^{\zeta k+1} \begin{Bmatrix} \{\overline{e}_{31}\} \\ \{\overline{e}_{32}\} \end{Bmatrix} \frac{\partial u_3}{\partial t} \, d\zeta$$

$$\equiv \begin{Bmatrix} \{A_{31}\} \\ \{A_{32}\} \end{Bmatrix} \frac{\partial u_3}{\partial t} \tag{26}$$

$$\begin{Bmatrix} \{M_1^M\} \\ \{M_2^M\} \end{Bmatrix} = \sum_{k=m_1,m_2\ldots}^{N} \int_{\zeta k}^{\zeta k+1} \begin{Bmatrix} \{\overline{e}_{31}\} \\ \{\overline{e}_{32}\} \end{Bmatrix} \zeta H_\zeta \, d\zeta$$

$$= ck_c \sum_{k=m_1,m_2\ldots}^{N} \int_{\zeta k}^{\zeta k+1} \begin{Bmatrix} \{\overline{e}_{31}\} \\ \{\overline{e}_{32}\} \end{Bmatrix} \frac{\partial u_3}{\partial t} \, \zeta \, d\zeta$$

$$\equiv \begin{Bmatrix} \{B_{31}\} \\ \{B_{32}\} \end{Bmatrix} \frac{\partial u_3}{\partial t} \tag{27}$$

$$\begin{Bmatrix} \{K_1^M\} \\ \{K_2^M\} \end{Bmatrix} = \sum_{k=m_1,m_2\ldots}^{N} \int_{\zeta k}^{\zeta k+1} \begin{Bmatrix} \{\overline{e}_{31}\} \\ \{\overline{e}_{32}\} \end{Bmatrix} \zeta^3 H_\zeta \, d\zeta$$

$$= ck_c \sum_{k=m_1,m_2\ldots}^{N} \int_{\zeta k}^{\zeta k+1} \begin{Bmatrix} \{\overline{e}_{31}\} \\ \{\overline{e}_{32}\} \end{Bmatrix} \frac{\partial u_3}{\partial t} \, \zeta^3 \, d\zeta$$

$$\equiv \begin{Bmatrix} \{C_{31}\} \\ \{C_{32}\} \end{Bmatrix} \frac{\partial u_3}{\partial t} \tag{28}$$

where

$$A_{ij} = ck_c \sum_{k=m_1,m_2\ldots} \overline{e}_{ij}^{(k)} (\zeta_{k+1} - \zeta_k), \quad i = 3 \; ; \; j = 1, 2$$

$$B_{ij} = \frac{1}{2} ck_c \sum_{k=m_1,m_2\ldots} \overline{e}_{ij}^{(k)} (\zeta_{k+1}^2 - \zeta_k^2), \quad i = 3 \; ; \; j = 1, 2$$

$$C_{ij} = \frac{1}{4} ck_c \sum_{k=m_1,m_2\ldots} \overline{e}_{ij}^{(k)} (\zeta_{k+1}^4 - \zeta_k^4), \quad i = 3 \; ; \; j = 1, 2 \tag{29}$$

and m_1, m_2, ... denote the layer numbers of the magnetostrictive or any actuating/sensing layers.

Analytical Solution

The equations of motion (18) can be expressed in terms of (u_1, u_2, u_3, ϕ_1, ϕ_2) displacements by substituting for the force and moment resultants from Eqs. (22,23). One can derive the equations of motion for homogeneous laminates.

Exact solution for the partial differential equations (18) on arbitrary domains and for general boundary conditions is not possible. However, for simply supported shells whose projection in the x_1, x_2-plane is a rectangle and for a lamination scheme of antisymmetric cross-ply or symmetric cross-ply type equations (18) are solved exactly. The Navier solution exists if the following stiffnesses are zero [23].

$$A_{i6} = B_{i6} = D_{i6} = E_{i6} = F_{i6} = H_{i6} = 0 \quad (i = 1, 2) \quad \text{and}$$
$$A_{45} = D_{45} = F_{45} = 0 \tag{30}$$

The simply-supported boundary conditions for the higher order shear deformation theory (HSDT) are assumed to be

$$u_1(x_1, 0, t) = 0, \quad u_1(x_1, b, t) = 0, \quad u_2(0, x_2, t) = 0, \quad u_2(a, x_2, t) = 0$$

$$u_3(x_1, 0, t) = 0, \quad u_3(x_2, b, t) = 0, \quad u_3(0, x_2, t) = 0, \quad u_3(a, x_2, t) = 0$$

$$N_1(0, x_2, t) = 0, \quad N_1(a, x_2, t) = 0, \quad N_2(x_1, 0, t) = 0, \quad N_2(x_1, b, t) = 0$$

$$M_1(0, x_2, t) = 0, \quad M_1(a, x_2, t) = 0, \quad M_2(x_1, 0, t) = 0, \quad M_2(x_1, b, t) = 0$$

$$P_1(0, x_2, t) = 0, \quad P_1(a, x_2, t) = 0, \quad P_2(x_1, 0, t) = 0, \quad P_2(x_1, b, t) = 0$$

$$\phi_1(x_1, 0, t) = 0, \quad \phi_1(x_1, b, t) = 0, \quad \phi_2(0, x_2, t) = 0, \quad \phi_2(a, x_2, t) = 0 \tag{31}$$

where a and b denote the lengths along x_1 and x_2 directions, respectively. The boundary conditions in equation (31) are satisfied by the following expansions (Reddy [21]).

$$u_1(x_1, x_2, t) = \sum_{n=1}^{\infty} \sum_{m=1}^{\infty} U_{mn}(t) \cos \alpha x_1 \sin \beta x_2$$

$$u_2(x_1, x_2, t) = \sum_{n=1}^{\infty} \sum_{m=1}^{\infty} V_{mn}(t) \sin \alpha x_1 \sin \beta x_2$$

$$u_3(x_1, x_2, t) = \sum_{n=1}^{\infty} \sum_{m=1}^{\infty} W_{mn}(t) \sin \alpha x_1 \sin \beta x_2$$

$$\phi_1(x_1, x_2, t) = \sum_{n=1}^{\infty} \sum_{m=1}^{\infty} X_{mn}(t) \cos \alpha x_1 \sin \beta x_2$$

$$\phi_2(x_1, x_2, t) = \sum_{n=1}^{\infty} \sum_{m=1}^{\infty} Y_{mn}(t) \sin \alpha x_1 \cos \beta x_2 \tag{32}$$

Substituting equation (32) into equations of motion (18) we obtain

$$\begin{bmatrix} S_{11} & S_{12} & S_{13} & S_{14} & S_{15} \\ S_{21} & S_{22} & S_{23} & S_{24} & S_{25} \\ S_{31} & S_{32} & S_{33} & S_{34} & S_{35} \\ S_{41} & S_{42} & S_{43} & S_{44} & S_{45} \\ S_{51} & S_{52} & S_{53} & S_{54} & S_{55} \end{bmatrix} \begin{Bmatrix} U_{mn} \\ V_{mn} \\ W_{mn} \\ X_{mn} \\ Y_{mn} \end{Bmatrix}$$

$$+ \begin{bmatrix} 0 & 0 & C_{13} & 0 & 0 \\ 0 & 0 & C_{23} & 0 & 0 \\ 0 & 0 & C_{33} & 0 & 0 \\ 0 & 0 & C_{43} & 0 & 0 \\ 0 & 0 & C_{53} & 0 & 0 \end{bmatrix} \begin{Bmatrix} \dot{U}_{mn} \\ \dot{V}_{mn} \\ \dot{W}_{mn} \\ \dot{X}_{mn} \\ \dot{Y}_{mn} \end{Bmatrix}$$

$$+ \begin{bmatrix} M_{11} & 0 & M_{13} & M_{14} & 0 \\ 0 & M_{22} & M_{23} & 0 & M_{25} \\ M_{31} & M_{32} & M_{33} & M_{34} & M_{35} \\ M_{41} & 0 & M_{43} & M_{44} & 0 \\ 0 & M_{52} & M_{53} & 0 & M_{55} \end{bmatrix} \begin{Bmatrix} \ddot{U}_{mn} \\ \ddot{V}_{mn} \\ \ddot{W}_{mn} \\ \ddot{X}_{mn} \\ \ddot{Y}_{mn} \end{Bmatrix} = \begin{Bmatrix} 0 \\ 0 \\ Q_{mn} \\ 0 \\ 0 \end{Bmatrix} \tag{33}$$

Where S_{ij}, C_{ij} and M_{ij} (i, j = 1,2, ... 5) are written in equations (39-41) in the appendix. For vibration control, we assume $q = 0$ and seek solution of the ordinary differential equations in the following form

$$U_{mn}(t) = U_0 e^{\lambda t}, \quad V_{mn}(t) = V_0 e^{\lambda t}, \quad W_{mn}(t) = W_0 e^{\lambda t},$$

$$X_{mn}(t) = X_0 e^{\lambda t}, \quad Y_{mn}(t) = Y_0 e^{\lambda t} \tag{34}$$

Substituting equation (34) into equation (33), for a non-trivial solution we obtain the result

$$\begin{bmatrix} \bar{S}_{11} & \bar{S}_{12} & \bar{S}_{13} & \bar{S}_{14} & \bar{S}_{15} \\ \bar{S}_{21} & \bar{S}_{22} & \bar{S}_{23} & \bar{S}_{24} & \bar{S}_{25} \\ \bar{S}_{31} & \bar{S}_{32} & \bar{S}_{33} & \bar{S}_{34} & \bar{S}_{35} \\ \bar{S}_{41} & \bar{S}_{42} & \bar{S}_{43} & \bar{S}_{44} & \bar{S}_{45} \\ \bar{S}_{51} & \bar{S}_{52} & \bar{S}_{53} & \bar{S}_{54} & \bar{S}_{55} \end{bmatrix} = 0 \tag{35}$$

where

$$\bar{S}_{ij} = S_{ij} + \lambda\, C_{ij} + \lambda^2 M_{ij} \text{ (for } \; i, j = 1, 2, 3, 4, 5 \text{)} \qquad (36)$$

This equation gives five sets of eigenvalues. The lowest one corresponds to the transverse motion. The eigenvalue can be written as $\lambda = -\alpha + i\,\omega_d$, so that the damped motion is given by

$$u_3 (x_1, x_2, t) = \frac{1}{\omega_d} e^{-\alpha t} \sin \omega_d t \sin \frac{n \pi x_1}{a} \sin \frac{n \pi x_2}{b} \qquad (37)$$

In arriving at the last solution, the following boundary conditions are used:

$$u_1 (x_1, x_2, 0) = 0, \quad \dot{u}_1 (x_1, x_2, 0) = 0, \quad u_2 (x_1, x_2, 0) = 0,$$

$$\dot{u}_2 (x_1, x_2, 0) = 0, \quad u_3 (x_1, x_2, 0) = 0, \quad \dot{u}_3 (x_1, x_2, 0) = 1,$$

$$\phi_1 (x_1, x_2, 0) = 0, \quad \dot{\phi}_1 (x_1, x_2, 0) = 0, \quad \phi_2 (x_1, x_2, 0) = 0,$$

$$\dot{\phi}_2 (x_1, x_2, 0) = 0 \qquad (38)$$

Results and Discussion

Numerical results are obtained using the formulation presented here and the results are obtained for natural frequencies, magnetostrictive damping coeffcients. The suppression time required to reduce vibration amplitudes to one-tenth of undamped values is calculated. The maximum amplitude occurs at the center of the shell panel for simply supported shells. Various lamination schemes are considered to show the influence of the position of the pair of magnetostrictive layers from the neutral plane on the amplitude suppression time. Also, a time ratio relation between the thickness of the layers and the distance to the neutral plane of the laminated composite shell is obtained. All values of the composite material and structural constants are tabulated and both damped and undamped frequencies are presented in the figures.

The material properties used are same as those used in [17]. The shell of arc lengths 1 m each is considered. The composite lamina material properties are listed in Table-1. Magnetostrictive material properties (for Terfenol-D material) are assumed to be

$$E_m = 26.5 \text{ GPa}, \quad \nu_m = 0.0, \quad \rho_m = 9250 \text{ kg} - \text{m}^{-3},$$

$$d_k = 1.67^{-8}\, m\text{A}^{-1}, \quad c\,(t)\, r_c = 10^4$$

k_c / r_c is assumed as 1. Magnetostrictive constants are calculated as

$$e_{31}^{(k)} = e_{32}^{(k)} = E_m * d_k / (2\,(1 + \nu_m))$$

The numerical values of various materials and structural constants (e.g. moment of inertia, magnetostrictive material constants) based on different lamination schemes and material properties (CFRP, Graphite-Epoxy (Gr-Ep) (AS), Glass-Epoxy (Gl-Ep), Boron-Epoxy (Br-Ep)) are listed in Tables 2-5. Numerical values of such constants based on classical and first order shear deformation theory are available in references [17, 26]. One needs to compare the values of these constants and debug the developed computer code.

Magnetostrictive damping coeffcients and natural frequencies for CFRP lamination schemes are listed in Tables 6-11. h_l , h_m and h represent the thickness of each composite layer, thickness of magnetostrictive layer and total thickness of the shell, respectively.

Tables-6 and 7 show the influence of the position of the magnetostrictive layer (in the $\zeta = z$-direction) from the neutral axis and the influence of the lamination scheme on the damping of amplitude of vibration for the fundamental mode, $(u_3)_{\max} \equiv w_c$ (maximum transverse deflection of the shell panel). The value of α [see Eq. (37)] increases when the magnetostrictive layer is located farther away from the neutral axis, indicating faster vibration suppression. This is due to the larger bending moment created by actuating force in the magnetostrictive layers. This effect can also be seen from Fig.3a-3e. Fig.4 contains a superposition of the results of $[\mathbf{m}/0/90/0/90]_s$, $[0/\mathbf{m}/90/0/90]_s$ and $[0/90/\mathbf{m}/90]_s$ lamination schemes. It is also observed from Fig.4 that $[\mathbf{m}/0/90/0/90]_s$ has has the maximum vibration suppression and thus the lowest frequency. Present results also show that the vibration suppression time decreases very rapidly as mode number increases. Fig.5 shows the transient response of modes 1 and 3 for a ten layered $[0/90/\mathbf{m}/0/90]_s$ laminate. Figs.6a-6d show the transient response of modes 1, 3, 5 and 7, respectively, for a ten layered $[0/90/\mathbf{m}/0/90]_s$ laminate. It can be observed that attenuation favors the higher modes. This is clearly seen in Fig.5, where modes 1 and 3 are superposed and it is obvious that mode 3 attenuates at a significantly faster rate.

Table-1 : Material Constants of Various Composite Materials

Material	E_{11} [GPa]	E_{22} [GPa]	G_{13} [GPa]	G_{23} [GPa]	G_{12} [GPa]	ν_{12}	ρ [$kg\,m^{-3}$]
CFRP	138.6	8.27	4.96	4.96	4.12	0.26	1824
Gr-Ep (AS)	137.9	8.96	7.20	6.21	7.20	0.30	1450
Gl-Ep	53.78	17.93	8.96	3.45	8.96	0.46	1900
Br-Ep	206.9	20.69	6.9	4.14	6.9	0.30	1950

Table-2 : Coefficients for Different Laminates and Materials

Material	Laminate	Z_m m	F_{11} Nm^3	H_{11} Nm^5 (10^{-5})	D_{11} Nm (10^4)	F_{12} Nm^3 (10^{-2})	H_{12} Nm^5 (10^{-7})
CFRP	$[0/90/0/90/\mathbf{m}]_s$	0.0005	0.132	0.257	0.768	0.270	0.482
	$[0/90/0/\mathbf{m}/90]_s$	0.0015	0.132	0.257	0.776	0.267	0.481
	$[0/90/\mathbf{m}/9/90]_s$	0.0025	0.06	0.116	0.357	0.013	0.025
	$[0/\mathbf{m}/90/0/90]_s$	0.0035	0.128	0.257	0.707	0.202	0.394
	$[\mathbf{m}/0/90/0/90]_s$	0.0045	0.068	0.104	0.527	0.088	0.101
Gr-Ep	$[0/90/\mathbf{m}/0/90]_s$	0.0025	0.123	0.250	0.685	0.315	0.588
Gl-Ep	$[0/90/\mathbf{m}/0/90]_s$	0.0025	0.06	0.116	0.357	0.131	0.024
Br-Ep	$[0/90/\mathbf{m}/0/90]_s$	0.0025	0.187	0.379	0.103	0.730	0.014

Table-3 : Coefficients for Different Laminates and Materials

Material	Laminate	D_{12} Nm (10^3)	F_{22} Nm^3 (10^{-1})	H_{22} Nm^5 (10^{-6})	D_{22} Nm (10^4)	F_{66} Nm^3 (10^{-2})	H_{66} Nm^5 (10^{-7})
CFRP	$[0/90/0/90/\mathbf{m}]_s$	0.179	0.529	0.721	0.454	0.515	0.919
	$[0/90/0/\mathbf{m}/90]_s$	0.170	0.515	0.717	0.526	0.526	0.923
	$[0/90/\mathbf{m}/9/90]_s$	0.153	0.529	0.727	0.424	0.592	0.973
	$[0/\mathbf{m}/90/0/90]_s$	0.127	0.272	0.336	0.289	0.800	1.290
	$[\mathbf{m}/0/90/0/90]_s$	0.921	0.368	0.583	0.318	0.128	2.530
Gr-Ep	$[0/90/\mathbf{m}/0/90]_s$	0.191	0.533	0.738	0.426	0.939	1.621
Gl-Ep	$[0/90/\mathbf{m}/0/90]_s$	0.792	0.381	0.613	0.277	0.116	2.025
Br-Ep	$[0/90/\mathbf{m}/0/90]_s$	0.443	0.853	0.123	0.657	0.916	1.578

In this study, the vibration suppression time is defined as the time required to reduce the uncontrolled vibration amplitude to one-tenth of its initial amplitude. Numerical simulations are carried out to estimate the vibration suppression time ratio (suppression time divided by the maximum suppression time) as the distance between the magnetostrictive layers and the neutral axis are varied. Parametric studies involving different lamination schemes, layer thickness and control gain values were carried out. Results are presented in Tables 6-10. Generally, the maximum suppression time is realized when the magnetostrictive layer is closest to the neutral axis of the shell. As a result of the normalization, Tables 8-9 show that the suppression time ratio does not change with the intensity of control gain of the magnetic field.

Table-4 : Coefficients for Different Laminates and Materials

Material	Laminate	D_{66} Nm (10^3)	F_{44} Nm^3 (10^{-2})	H_{44} Nm (10^3)	A_{44} Nm^{-1} (10^8)	F_{55} Nm^3 (10^{-2})	D_{55} Nm^5 (10^3)
CFRP	$[0/90/0/90/\mathbf{m}]_s$	0.349	0.621	0.419	0.662	0.621	0.419
	$[0/90/0/\mathbf{m}/90]_s$	0.386	0.630	0.452	0.662	0.630	0.452
	$[0/90/\mathbf{m}/9/90]_s$	0.459	0.690	0.518	0.662	0.690	0.518
	$[0/\mathbf{m}/90/0/90]_s$	0.568	0.879	0.618	0.662	0.879	0.618
	$[\mathbf{m}/0/90/0/90]_s$	0.715	1.317	0.750	0.662	1.317	0.750
Gr-Ep	$[0/90/\mathbf{m}/0/90]_s$	0.670	0.863	0.629	0.797	0.912	0.647
Gl-Ep	$[0/90/\mathbf{m}/0/90]_s$	0.801	0.686	0.551	0.761	0.984	0.661
Br-Ep	$[0/90/\mathbf{m}/0/90]_s$	0.655	0.681	0.530	0.707	0.830	0.585

Table-5 : Coefficients for Different Laminates and Materials

Material	Laminate	I_1 kgm^{-2} (10^2)	I_3 kg (10^{-3})	I_5 kgm^2 (10^{-8})	I_7 kgm^4 (10^{-13})	$-B_{31}$ (10^2)	$-C_{31}$ (10^{-4})
CFRP	$[0/90/0/90/\mathbf{m}]_s$	0.331	0.157	0.228	0.407	0.044	0.022
	$[0/90/0/\mathbf{m}/90]_s$	0.331	0.187	0.237	0.410	0.133	0.332
	$[0/90/\mathbf{m}/9/90]_s$	0.331	0.246	0.291	0.451	0.221	1.438
	$[0/\mathbf{m}/90/0/90]_s$	0.331	0.335	0.460	0.708	0.310	3.872
	$[\mathbf{m}/0/90/0/90]_s$	0.331	0.454	0.852	1.717	0.398	8.165
Gr-Ep	$[0/90/\mathbf{m}/0/90]_s$	0.331	0.246	0.291	0.451	0.221	1.438
Gl-Ep	$[0/90/\mathbf{m}/0/90]_s$	0.331	0.246	0.291	0.451	0.221	1.438
Br-Ep	$[0/90/\mathbf{m}/0/90]_s$	0.331	0.246	0.291	0.451	0.221	1.438

Table-6 : Suppression Time Ratio for Different CFRP Laminates of Total Thickness h = 10mm; h_l = 1mm and h_m = 1mm

Laminate	Z_m (m)	$-\alpha$	$\pm\omega_d$	W_{max} (mm)	t at $W_{max}/10$	T_s
$[0/90/0/90/\mathbf{m}]_s$	0.0005	1.318	214.522	4.612	1.764	1.000
$[0/90/0/\mathbf{m}/90]_s$	0.0015	3.954	215.376	4.507	0.591	0.337
$[0/90/\mathbf{m}/9/90]_s$	0.0025	6.590	212.563	4.477	0.362	0.215
$[0/\mathbf{m}/90/0/90]_s$	0.0035	9.226	205.508	4.539	0.283	0.152
$[\mathbf{m}/0/90/0/90]_s$	0.0045	11.864	191.557	4.745	0.205	0.117

In all the numerical simulations the suppression time ratio is given by $h_m/(2\,z_m)$, where h_m is the thickness of the magnetostrictive layer and z_m is the distance between the magnetostrictive layer and the mid-plane of the shell. The normalized suppression time is denoted as T_s.

From Figs.3-4, it is observed that the damping increases as the magnetostrictive layers are moved away from the neutral axis. From Tables 6-10, we examined the variation of the time ratio with respect to the distance of the magnetostrictive layer from the neutral axis for various lamination schemes and magnetostrictive layer thick-

Table-7 : Suppression Time Ratio for Different CFRP Laminates, h = 44mm; h_l = 5mm and h_m = 2mm

Laminate	Z_m (m)	-α	$\pm\omega_d$	W_{max} (mm)	t at $W_{max}/10$	T_s
$[0/90/0/90/\mathbf{m}]_s$	0.001	1.536	1084.358	0.919	1.502	1.000
$[0/90/0/\mathbf{m}/90]_s$	0.006	9.216	1079.978	0.912	0.252	0.168
$[0/90/\mathbf{m}/9/90]_s$	0.011	16.901	1070.491	0.910	0.143	0.095
$[0/\mathbf{m}/90/0/90]_s$	0.016	24.627	1057.490	0.911	0.065	0.095
$[\mathbf{m}/0/90/0/90]_s$	0.021	32.519	1015.837	0.936	0.075	0.050

Table-8 : Suppression Time Ratio for Control Gain (10^4) for Different Locations of Magnetostrictive Layers in CFRP Laminated Shell, h = 50mm; h_l = 5mm and h_m = 5mm

Laminate	Z_m (m)	$C(t)\ r_C = 10^4$				
		-α	$\pm\omega_d$	W_{max} (mm)	t (s)	T_s
$[0/90/0/90/\mathbf{m}]_s$	0.0025	6.376	1067.206	0.928	0.366	1.000
$[0/90/0/\mathbf{m}/90]_s$	0.0075	19.115	1057.390	0.919	0.126	0.344
$[0/90/\mathbf{m}/9/90]_s$	0.0125	31.832	1038.613	0.918	0.074	0.202
$[0/\mathbf{m}/90/0/90]_s$	0.0175	44.575	1012.998	0.922	0.051	0.139
$[\mathbf{m}/0/90/0/90]_s$	0.0225	57.648	940.434	0.963	0.042	0.115

Table-9 : Suppression Time Ratio for Control Gain (10^3) for Different Locations of Magnetostrictive Layers in CFRP Laminated Shell, h = 50mm; h_l = 5mm and h_m = 5mm

Laminate	Z_m (m)	$C(t)\ r_C = 10^3$				
		-α	$\pm\omega_d$	W_{max} (mm)	t (s)	T_s
$[0/90/0/90/\mathbf{m}]_s$	0.0025	0.638	1067.224	0.936	3.616	1.000
$[0/90/0/\mathbf{m}/90]_s$	0.0075	1.912	1057.561	0.943	1.207	0.334
$[0/90/\mathbf{m}/9/90]_s$	0.0125	3.183	1039.096	0.958	0.727	0.201
$[0/\mathbf{m}/90/0/90]_s$	0.0175	4.457	1013.968	0.978	0.522	0.144
$[\mathbf{m}/0/90/0/90]_s$	0.0225	5.765	942.181	1.039	0.402	0.111

nesses. When one compare the Tables-7 and 10 one can observe that the convergence rate of the maximum amplitude is faster in thinner magnetostrictive layer. Thus a relatively thinner magnetostrictive layer leads to better attenuation characteristics.

Vibration frequencies for the thin and thick shells are obtained using FSDT and HSDT and listed in Table-11. For an a/h ratio of 10 HSDT predicted 23 per cent larger amplitude W_{max} as compared to FSDT. Vibration suppression results are shown in Fig.7. It is observed that for thicker shells HSDT predicts larger amplitude of vibration and longer vibration suppression time as compared to FSDT predictions. This is attributed to the fact that HSDT include the shear deformation component more appropriately.

Conclusions

Analytical solution for simply supported composite shells with smart material layers embedded in them is presented in this study. The third-order shell theory is used

Table-10 : Suppression Time Ratio for Different CFRP Laminates, h = 30mm; h_l = 3mm and h_m = 3mm

Laminate	Z_m (m)	$-\alpha$	$\pm\omega_d$	W_{max} (mm)	t at $W_{max}/10$	T_s
$[0/90/0/90/\mathbf{m}]_s$	0.0015	3.910	646.233	1.533	0.595	1.000
$[0/90/0/\mathbf{m}/90]_s$	0.0045	11.729	640.277	1.518	0.208	0.349
$[0/90/\mathbf{m}/9/90]_s$	0.0075	19.541	629.287	1.514	0.122	0.205
$[0/\mathbf{m}/90/0/90]_s$	0.0105	27.359	615.277	1.517	0.094	0.158
$[\mathbf{m}/0/90/0/90]_s$	0.0135	35.251	570.460	1.594	0.069	0.116

Table-11 : Comparison of Shell Results Obtained Using FSDT and HSDT

a/h	W_{max} (FSDT) (mm)	t (FSDT) (s)	W_{max} (HSDT) (mm)	t (HSDT) (s)	% Difference W_{max}
10	0.742	0.078	0.918	0.074	23.7
100	4.440	0.355	4.447	0.362	0.8

to study vibration suppression characteristics. The analytical solution is based on the Navier solution procedure. The velocity feedback control is used. The smart material used in this study to achieve vibration suppression of laminated composite shells is the Terfenol-D magnetostrictive material. The vibration suppression characteristics of laminated shells are studied for a number of different cases and the results are presented in tables and figures.

The effect of placing the smart material layer at various laminate positions with respect to the neutral axis of the shell has been studied. It has been found that there is maximum vibration suppression when the smart material layers are placed farthest from the neutral axis, which creates larger bending by the smart material layer. It has also been found that using thinner smart material layers have better vibration attenuation characteristics. The effect of using different values of the control gain has also been studied. It is observed that for a lower value of the control gain the time taken to suppress the vibration is longer. This is expected, as the amount of actuation done by the smart material layer onto the composite shell is less as the feedback value is less. For thicker shells HSDT predicts larger amplitude of vibration and longer vibration suppression time as compared to FSDT predictions.

References

1. Uchino, K.,"Electrostrictive Actuators: Materials and Applications", Ceramics Bulletin, 1986, Vol. 65, pp. 647-652.

2. Cross, L.E. and Jang, S.J.,"Electrostrictive Materials", Proceedings of "Recent Advances in Piezoelectric Ceramics, Electronic Ceramics, Properties, Devices, and Applications", Marcel Dekker, Inc., New York, 1988, pp. 129-137.

3. Crawley, E.F. and Luis, J.D.,"Use of Piezoelectric actuators and Elements of Intelligent Structure". AIAA Journal, 1987, Vol 25, pp. 1373-1385.

4. Baz, A., Imam, K. and Mccoy, J.,"The Dynamics of Helical Shape Memory Actators". Journal of Intelligent Material Systems and Structures, 1990, Vol.1, pp.105-133.

5. Choi, Y., Sprecher, A.F. and Conrad, H.,"Vibration Characteristics of a Composite Beam Containing Electrorheological Fluid", Journal of Intelligent Material Systems and Structures, 1990, Vol.1, pp.91-104.

6. Goodfriend, M.J. and Shoop, K.M.,"Adaptive Characteristics of the Magnetostrictive Alloy, Terfenol-D, for Active Vibration Control", Journal of Intelligent Material Systems and Structures, 1992, Vol. 3, pp. 245-254.

7. Bryant, M.D., Fernandez, B. and Wang, N.,"Active Vibration Control in Structures Using Magnetostrictive Terfenol with Feedback and/or Neural Network

Controllers", Journal of Intelligent Material Systems and Structures, 1993, Vol. 4, pp. 484-489.

8. Friedmann, P.P., Carman, G.P. and Millott, T.A.,"Magnetostrictively Actuated Control Flaps for Vibration Reduction in Helicopter Rotors - Design Considerations for Implementation", Mathematical and Computer Modelling, 2001, Vol. 33, (10-11) pp.1203-1217.

9. Anjanappa, M. and Bi, J., " A Theoretical and Experimental Study of Magnetostrictive Mini Actuators", Smart Materials and Structures, 1994, Vol.1, pp.83-91.

10. Anjanappa, M. and Bi, J.,"Magnetostrictive Mini Actuators for sMart Structural Application", Smart Materials and Structures, 1994, Vol.3(4), pp.383-390.

11. Pratt, J. R. and Flatau, A. B., "Development and Analysis of Self-sensing Magnetostrictive Actuator Design", Journal of Intelligent Material Systems and Structures, 1995, Vol.6, pp.639-648.

12. Eda, H., Kobayashi, T., Nakamura, H. and Akiyama, T., "Giant Magnetostriction Compounds with Structure Textured by Resin Bound on Giant Magnetostriction Fine Powder in Magnetic Field and its Actuator", Transactions of Japanese Society for Mechanical Engineering, Series C, 1995, Vol.61, pp.168-217.

13. Krishna Murty, A.V., Anjanappa, M. and Wu, Y. -F., "The Use of Magnetostrictive Particle Actuators for Vibration Attenuation of Flexible Beams", Journal of Sound and Vibration, 1997, Vol. 206 (2), pp.133-149.

14. Krishna Murty, A.V., Anjanappa, M., Wu, Y-F., Bhattacharya, B. and Bhat, M. S., "Vibration Suppression of Laminated Composite Beams Using Embedded Magnetostrictive Layers", Journal of Aeronautical Society of India, 1998, Vol.78, pp.38-44.

15. Reddy, J.N., "On Laminated Composite Plates with Integrated Sensors and Actuators", Engineering Structures, 1999, Vol. 21, pp.568-593.

16. Reddy, J.N. and Barbosa, J.A., "Vibration Suppression of Laminated Composite Beams", Smart Materials and Structures, 2000, Vol. 9, pp. 49-58.

17. Pradhan, S.C., Ng, T.Y., Lam, K.Y. and Reddy, J.N., "Control of Laminated Composite Plates Using Magnetostrictive Layers", Smart Materials and Structures, 2001, Vol. 10(4), pp. 657-667.

18. Marfia, S, Sacco, E. and Reddy, J. N., "Superelastic and Shape Memory Effects in Laminated SMA Beams", AIAA Journal, 2003, Vol. 41, pp.100-109.

19. Reddy, J. N. and Liu, C. F., "A Refined Shear Deformation Theory of Laminated Shells", International Journal of Engineering Science, 1985, Vol. 23, (3), pp. 319-330.

20. Reddy, J.N., "Energy and Variational Methods in Applied Mechanics", John Wiley & Sons, New York, 1985.

21. Reddy, J.N., "Mechanics of Laminated Composite Plates, Theory and Analysis", Boca Raton, FL: Chemical Rubber Company, 1997.

22. Reddy, J.N., "Exact Solutions of Moderately Thick Laminated Shells", Journal of Engineering Mechanics ASCE 1984, Vol. 110 (5), pp. 794-809.

23. Reddy, J. N., "A Refined Nonlinear Theory of Plates with tRansverse Shear Deformation", International Journal of Solids and Structures, 1984, Vol. 20 (9-10), pp. 881-893.

24. Lee, Y. Y. and Guo, X.,"Non-linear Vibration Suppression of a Composite Panel Subject to Random Acoustic Excitation Using Piezoelectric Actuators", Mechanical Systems and Signal Processing, 2007, Vol. 21(2), pp.1153-1173.

25. Song, G., Sethi, V. and Li, H. N.,"Vibration Control of Civil Structures Using Piezo-ceramic Smart Materials: A Review", Engineering Structures, 2006, Vol. 28(11), pp.1513-1524.

26. Pradhan, S.C., "Vibration Suppression of FGM Composite Shells Using Embedded Magnetostrictive Layers", International Journal of Solids and Structures, 2005, Vol .42,(9-10), pp. 2465-2488.

27. Zhang, H. Y. and Shen, Y. P.,"Vibration Suppression of Laminated Plates with 13 Piezoelectric Fiber-reinforced Composite Layers Equipped with Interdigitated Electrodes", Composite Structures, 2007, Vol.79(2), pp. 220-228.

Appendix

$$S_{11} = A_{11}\alpha^2 + A_{66}\beta^2$$

$$S_{12} = A_{12}\alpha\beta + A_{66}\alpha\beta$$

$$S_{13} = -A_{11}\frac{1}{R_1}\alpha - A_{12}\frac{1}{R_2}\alpha - C_1 E_{11}\alpha^3 - C_1 E_{12}\alpha\beta^2 - C_1 E_{66}2\alpha\beta^2$$

$$S_{14} = B_{11}\alpha^2 - C_1 E_{11}\alpha^2 + B_{66}\beta^2 - C_1 E_{66}\beta^2$$

$$S_{15} = B_{12}\alpha\beta - C_1 E_{12}\alpha\beta + B_{66}\alpha\beta - C_1 E_{66}\alpha\beta$$

$$S_{21} = S_{12}$$

$$S_{22} = A_{66}\alpha^2 + A_{22}\beta^2$$

$$S_{23} = -2C_1 E_{66}\alpha^2\beta - A_{12}\frac{1}{R_1}\beta - A_{22}\frac{1}{R_2}\beta - C_1 E_{12}\alpha^2\beta - C_1 E_{22}\beta^3$$

$$S_{24} = B_{66}\alpha\beta - C_1 E_{66}\alpha\beta + B_{12}\alpha\beta - C_1 E_{12}\alpha\beta$$

$$S_{25} = B_{66}\alpha^2 - C_1 E_{66}\alpha^2 + B_{22}\beta^2 - C_1 E_{22}\beta^2$$

$$S_{31} = S_{13}$$

$$S_{32} = S_{23}$$

$$S_{33} = A_{55}\alpha^2 - 2C_2 D_{55}\alpha^2 + A_{44}\beta^2 - 2C_2 D_{44}\beta^2 + C_2^2 F_{55}\alpha^2 + C_2^2 F_{44}\beta^2 + 2C_1 E_{11}\frac{1}{R_1}\alpha^2 + 2C_1 E_{12}\frac{1}{R_2}\alpha^2 + C_1^2 H_{11}\alpha^4 + C_1^2 H_{12}\alpha^2\beta^2 + 2C_1^2 H_{66}\alpha^2\beta^2 + 2C_1 E_{12}\frac{1}{R_1}\beta^2 + 2C_1 E_{22}\frac{1}{R_2}\beta^2 + C_1^2 H_{12}\alpha^2\beta^2 + C_1^2 H_{22}\beta^4 - A_{11}\frac{1}{R_1^2} - 2\frac{1}{R_1 R_2}A_{12} - A_{22}\frac{1}{R_2^2}$$

$$S_{34} = A_{55}\alpha - 2C_2 D_{55}\alpha + C_2^2 F_{55}\alpha - C_1 F_{11}\alpha^3 + C_1^2 H_{11}\alpha^3 - 2C_1 F_{66}\alpha\beta^2 + 2C_1^2 H_{66}\alpha\beta^2 + C_1^2 H_{12}\alpha\beta^2 - \frac{1}{R_1}B_{11}\alpha + C_1\frac{1}{R_1}E_{11}\alpha - \frac{1}{R_2}B_{12}\alpha + C_1\frac{1}{R_2}E_{12}\alpha$$

$$S_{35} = A_{44}\beta - 2C_2 D_{44}\beta + C_2^2 F_{44}\beta - C_1 F_{12}\alpha^2\beta + C_1^2 H_{12}\alpha^2\beta - 2C_1 F_{66}\alpha^2\beta + 2C_1^2 H_{66}\alpha^2\beta - C_1^2 F_{22}\beta^3 + C_1^2 H_{22}\beta^3 - \frac{1}{R_1}B_{12}\beta + C_1\frac{1}{R_1}E_{12}\beta - \frac{1}{R_2}B_{22}\beta + C_1\frac{1}{R_2}E_{22}\beta$$

$$S_{41} = S_{14}$$

$$S_{42} = S_{24}$$

$$S_{43} = S_{34}$$

$$S_{44} = D_{11}\alpha^2 - 2C_1 F_{11}\alpha^2 + D_{66}\beta^2 - 2C_1 F_{66}\beta^2 - A_{55} + 2C_2 D_{55} - C_2^2 F_{55} + C_1^2 H_{11}\alpha^2 + C_1^2 H_{66}\beta^2$$

$$S_{45} = D_{66}\alpha\beta + D_{12}\alpha\beta - 2C_1 F_{66}\alpha\beta - 2C_1 F_{12}\alpha\beta + C_1^2 H_{12}\alpha\beta - C_1 F_{66}\alpha\beta + C_1^2 H_{66}\alpha\beta$$

$$S_{51} = S_{15}$$

$$S_{52} = S_{25}$$

$$S_{53} = S_{35}$$

$$S_{54} = S_{45}$$

$$S_{55} = D_{66}\alpha^2 - 2C_1 F_{66}\alpha^2 + D_{22}\beta^2 - 2C_1 F_{22}\beta^2 - A_{44} + 2C_2 D_{44} - C_2^2 F_{44} + C_1^2 H_{66}\alpha^2 + C_1^2 H_{22}\beta^2 \tag{39}$$

$$C_{13} = A_{31}\alpha$$

$$C_{23} = A_{32}\beta$$

$$C_{33} = -C_{31}\alpha^2 - C_{32}\beta^2 + \frac{A_{31}}{R_1} + \frac{A_{32}}{R_2}$$

$$C_{43} = B_{31}\,\alpha - C_1\,C_{31}\,\alpha$$

$$C_{53} = B_{32}\,\beta - C_1\,C_{32}\,\beta \qquad (40)$$

$$M_{11} = \bar{I}_1$$

$$M_{12} = 0$$

$$M_{13} = \bar{I}_3\,\alpha$$

$$M_{14} = \bar{I}_2$$

$$M_{15} = 0$$

$$M_{21} = 0$$

$$M_{22} = \bar{J}_1$$

$$M_{23} = \bar{J}_3\,\beta$$

$$M_{24} = 0$$

$$M_{25} = \bar{J}_2$$

$$M_{31} = M_{13}$$

$$M_{32} = M_{23}$$

$$M_{33} = \bar{I}_1 + C_1^2\,I_7\,(\alpha^2 + \beta^2)$$

$$M_{34} = \bar{I}_5\,\alpha$$

$$M_{35} = \bar{J}_5\,\beta$$

$$M_{41} = M_{14}$$

$$M_{42} = 0$$

$$M_{43} = M_{34}$$

$$M_{44} = \bar{I}_4$$

$$M_{45} = 0$$

$$M_{51} = 0$$

$$M_{52} = M_{25}$$

$$M_{53} = M_{35}$$

$$M_{54} = 0$$

$$M_{55} = \bar{J}_4 \qquad (41)$$

where the magnetostrictive coefficients $A_{31}, A_{32}, B_{31}, B_{32}, C_{31}$ and C_{32} are defined in equation (27).

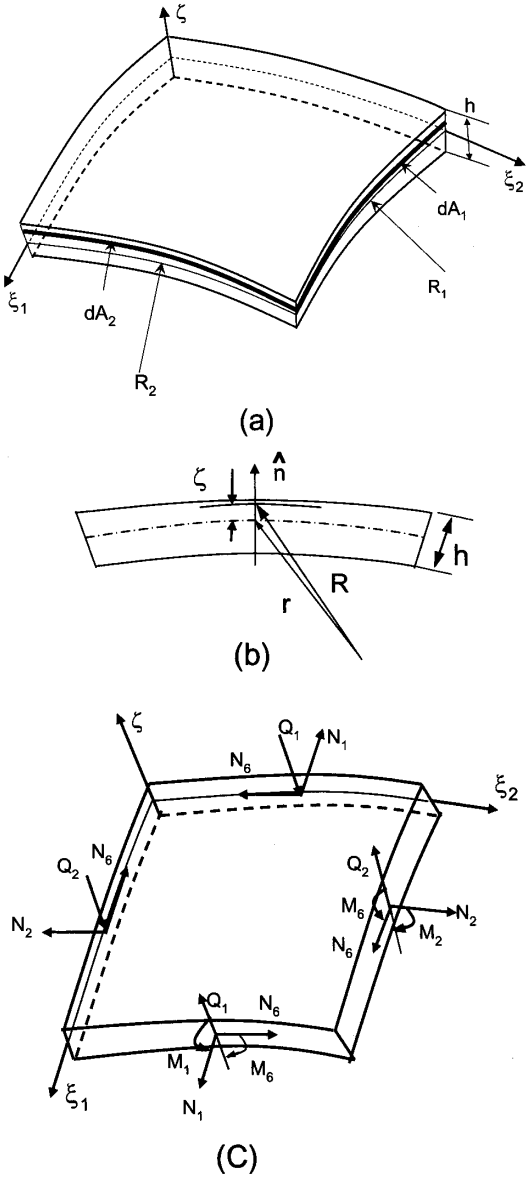

Fig.1 Geometry and Stress Resultants of Doubly Covered Shell

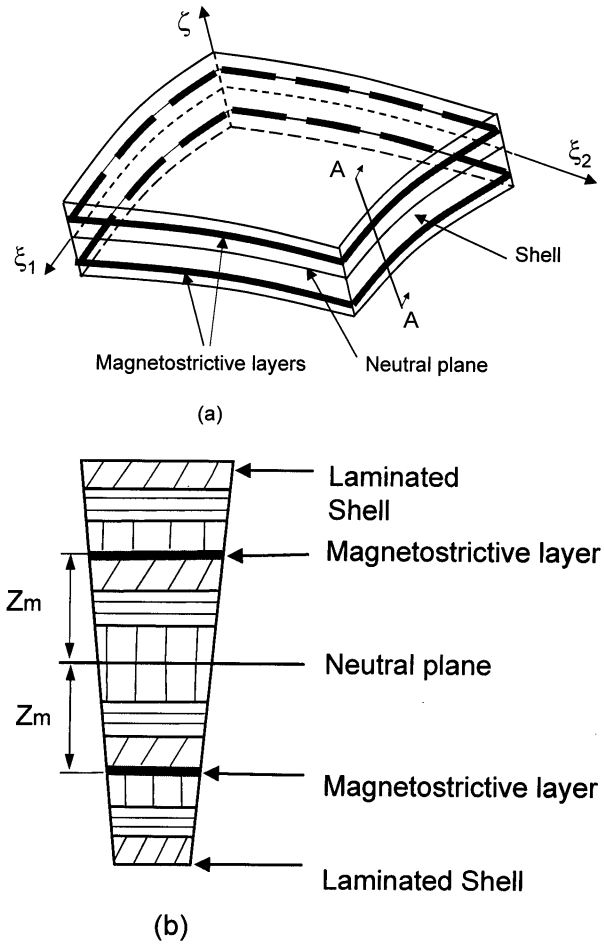

Fig.2 Laminated Shell with Embedded Magnetostrictive Layers with an Exploded View

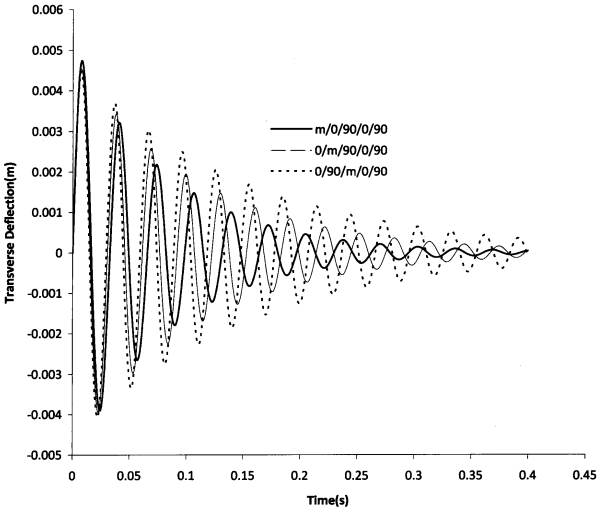

Fig.4 Controlled Motion at the Mid Point of Plate for Different Lamination Schemes

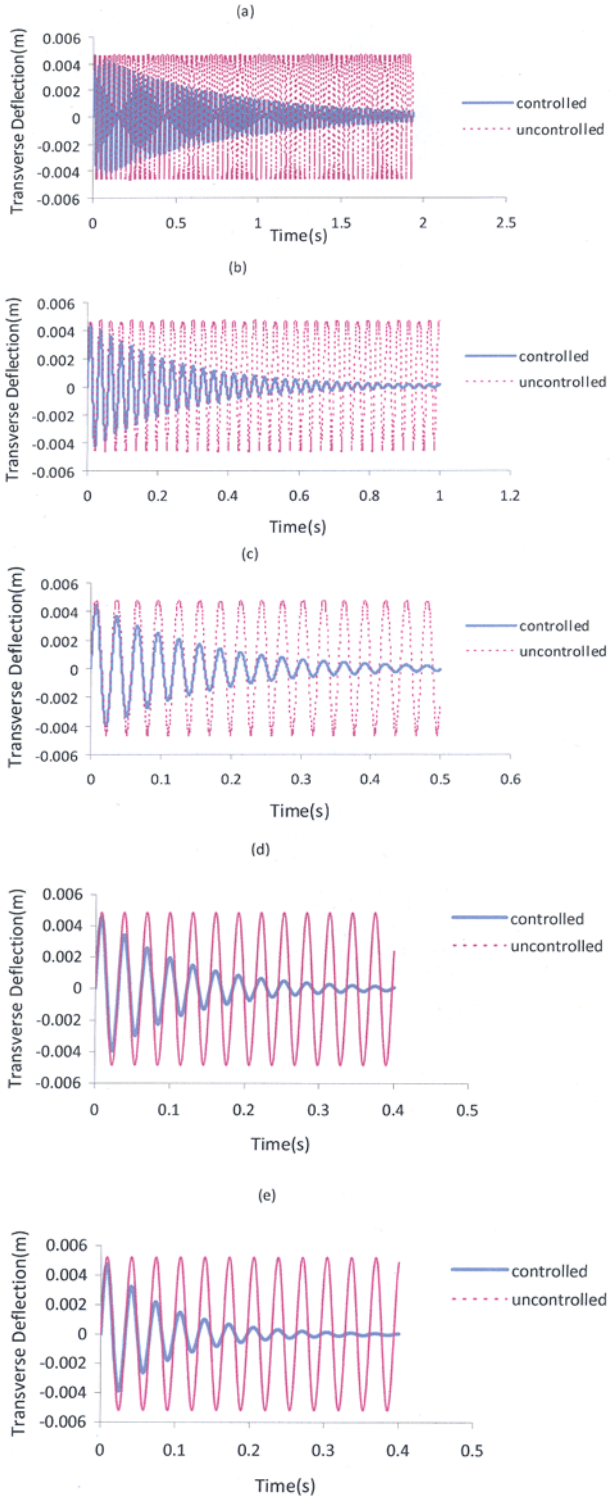

Fig.3 Comparison of Uncontrolled and Controlled Motion at the Midpoint of the CFRP Laminates for Various Locations of Magnetrostrictive Layers, (a) 0/90/0/90/m, (b) 0/90/0/m/90, (c) 0/90/m/0/90, (d) 0/m/90/0/90 and (e) m/0/90/0/90

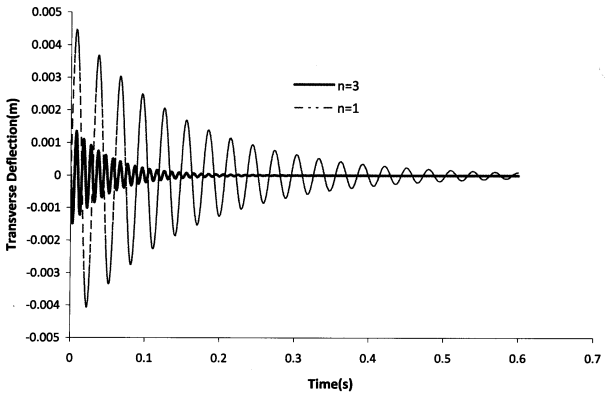

Fig.5 Comparison of Controlled Motion at the Midpoint of the CFRP Shells for Vibration Modes n = 1 and n = 3

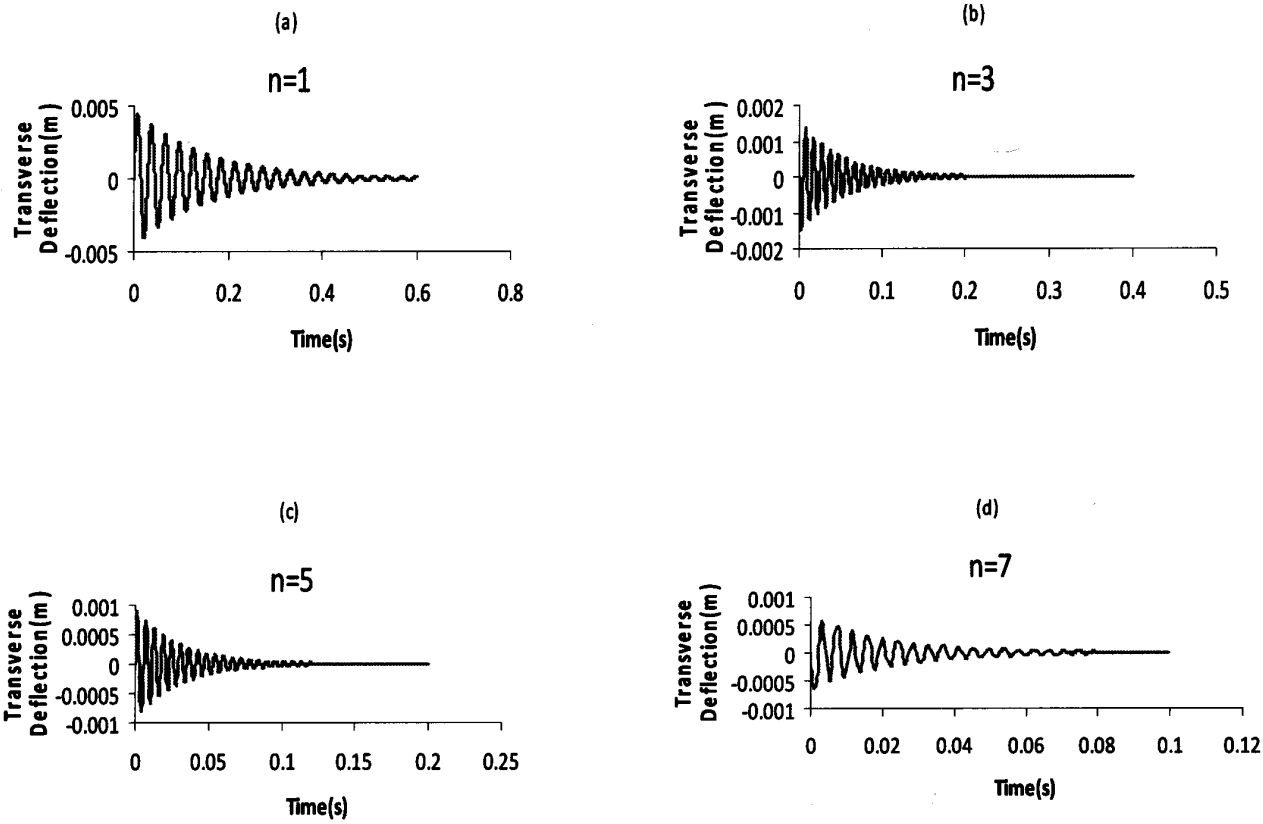

Fig.6 Vibration Suppression of Higher Modes at the Midpoint of the CFRP Shell (a) n = 1, (b) n = 3, (c) n = 5 and (d) n = 7

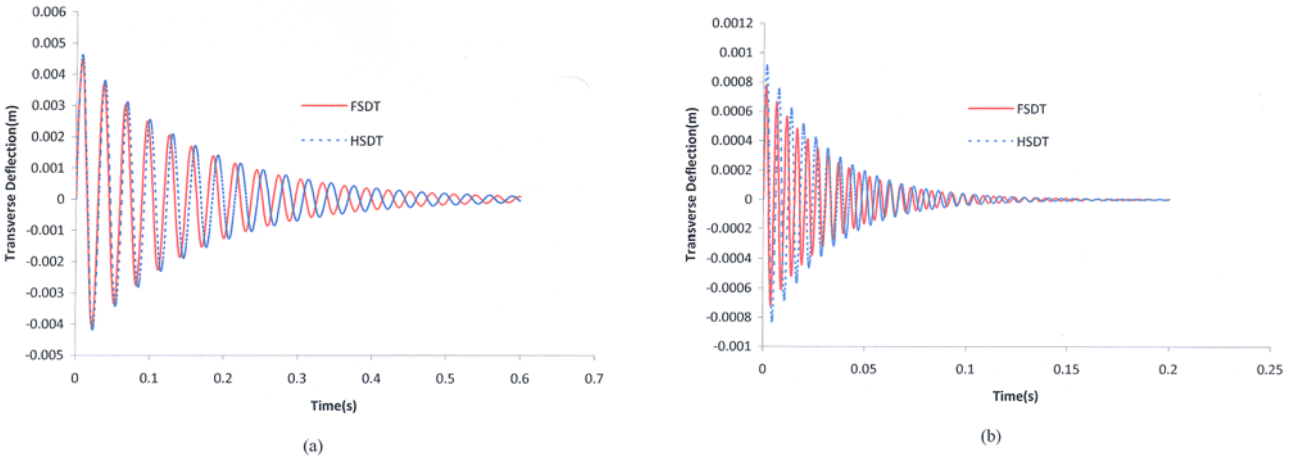

Fig.7 Comparison of HSDT and FSDT for Various a/h Ratios (a) 100 and (b) 10